

# Identifying the Location of Cracks in Intelligent Carbon Based TRC Elements

---

MAHDI GABEN and YISKA GOLDFELD

## ABSTRACT

The goal of the study is to develop an identification procedure that identifies the location of cracks within textile reinforced concrete (TRC) elements by using their smart self-sensory capabilities. To answer this goal the investigation offers to adopt the principles of the time domain reflectometer (TDR) analysis and to explore the changes of the spectrum of the impedance. In order to use the concept, the study considers the electrical characterization of the sensory carbon yarns, mainly the dependency of the impedance with the yarn's length and offers a calibration procedure. It was found that the procedure has the capabilities to identify all cracking events but also involved additional false alarm scenarios. It is further demonstrated that only the location of the first crack was accurately identified.

## INTRODUCTION

In the last decades, there has been an increasing need for intelligent, hybrid and sustainable structural elements. The technology of carbon-based textile reinforced concrete (TRC), which combines high performance cement with a high strength reinforcement system and inherent sensory capabilities, can answer this purpose [1-10]. The textile mesh is characterized by a high resistance to corrosion, which enables the construction of thin, light, and durable concrete elements [11-13]. Studies in the literature demonstrated the potential of using the TRC structures as smart hybrid structures and suggested to use their sensory capabilities to monitor the applied load [1, 2-3], to detect the occurrence of cracks [5], to estimate the integrative strain [5-6, 9-10] and to identify infiltration of water through cracked zones [14-15]. The monitoring systems were based on either direct current (DC) based or alternating current (AC) based systems [2-3, 5-8].

The DC-based systems used simple DC circuits [15] or Wheatstone bridge configurations [5-7] and correlated between electrical resistance and structural parameters. The AC electrical setups were based on utilizing the electrical properties of the system for the monitoring procedure [2-3, 8]. Although the monitoring systems were able to successfully correlate between the measured electrical properties and the structural or functional health, the obtained information was based on integrative measurements. This means that the location of the damage, such as cracks, could not be identified and remains an unknown parameter. Therefore, the goal of this study is to develop an identification procedure that has the capability to identify damaged zones along the TRC structures.

The study suggests adopting the concept of time domain reflectometer (TDR) to answer this goal. The concept is commonly used in coaxial. The monitoring concept is based on sending an energy pulse and measuring the reflected signals. Opposed to coaxial cables that are characterized by a constant electrical impedance and a constant velocity coefficient, carbon yarns are characterized by impedance that is dependent on the yarn's length [2-4], and its velocity coefficient is unknown and dependent on the health of the yarn. Furthermore, due to cracking, the filaments within the yarns gradually degrade. First the sleeve filaments break and then the core-inner filaments pull out. This unique irreversible micro-structural mechanism results in changing the current density distribution along the yarn [12]. Therefore, adopting the TDR concept for smart carbon based TRC element is not a straightforward act.

To handle these challenges the study offers an identification procedure in which two parallel carbon yarns are connected from one end to the data acquisition system. The study argues that since crack yields to local change of the impedance, it can be identified by measuring the changes of the spectrum of the impedance. Based on this hypothesis, the study develops a special TDR based identification procedure. The study presents the capabilities of the identification procedure by experimentally investigating textile reinforced magnesium phosphate cement (MPC) beams under uniaxial loading. Choosing MPC matrix, instead of conventional Portland cement (PC) based matrix, is mainly due to its enhanced mechanical and electrical properties [3, 7].

## **MATERIAL AND METHOD**

The study uses a generic carbon-based textile as the main reinforcement system of the MPC based beams. The geometry of the beams, the mechanical and electrical properties and the matrix, the smart reinforcement system, and the experimental setup are presents in this section.

### **Carbon-based textile mesh**

The study uses carbon yarns as the smart sensory agent. In the longitudinal direction ( $0^\circ$ ), six carbon yarns are positioned, and in the transverse direction ( $90^\circ$ ) AR-glass yarns are positioned. Using electrically insulated yarns, such as AR-glass yarns, aims to avoid electrical linkage between the sensory carbon yarns. The textile stitch is pillar, and its grip structure is warp-knitted with a mesh size of 7-8 mm. The mechanical and electrical properties of the yarns are given in [2, 3]. Each carbon yarn is characterized

by a RL electrical circuit with the following electrical properties:  $R_X=0.22+0.015X_{[\text{mm}]}$  [ $\Omega$ ],  $L_X=826+1.54X_{[\text{mm}]}$  [nH], where X is the yarn's length.

### **MPC matrix**

The study uses a commercial magnesium phosphate cement (MPC) matrix, produced by ICL Group Ltd. Generally, MPC is a production of acid-based solution, dead burnt magnesia, potassium-based phosphate and ammonium-based phosphate [3, 7]. Short aramid fibers (AF) were added to improve the ductility of the matrix [3, 7]. The study uses AF produced by Teijin Frontier company Ltd, its commercial name is Technora CF320. The short AF are 3 mm long, and they are electrically insulated. Further mechanical details can be found in [3]. The volume fraction of the fibers was specified as 0.5% and they were added to the water before the mixing process. The MPC matrix was prepared with a ratio of 1:4 water to dry material.

The mechanical properties of the MPC with the additive AF are determined according to EN 196-1:2005 at the age of 14 days. The tensile and compression strengths are  $6.6 \pm 0.43$  MPa and  $62 \pm 6.2$  MPa, respectively.

The electrical properties of the matrix were investigated in [3]. It was found that the MPC matrix is characterized by an increasing impedance and its value at 14 days is 35,443  $\Omega/\text{m}$  at a frequency of 1 MHz.

### **Loading setup of carbon-based textile reinforced MPC beams**

MPC beams were tested under tensile uniaxial loading procedure. The geometry of the beams are: 500 mm long, 50 mm wide and 8 mm thick. A single textile layer is poisoned in the middle of the cross-section of the beam.

The beam was loaded at a displacement rate of 0.5 mm/min using Instron model 5966 (10 kN load-cell capacity). Aluminum plates (90 or 170 mm long, 50 mm wide, 1.5 mm thick) were glued to the specimens' edges to avoid local stress and to provide a sufficient grip to the loading machine. Along the loading process, the applied displacement, the load, the crack propagation using the digital image correlation (DIC) technique, and the impedance spectrum were continuously monitored. Results from the DIC technique were analyzed by the commercial software LaVision DaVis 10. The loading setup is presented in Fig. 1.

### **SENSORY CONCEPT**

The monitoring procedure adopts the principles of the TDR analysis. It is based on sending energy pulses (by an electrical current, in our case by Fieldfox Handheld Analyzer N9918B with a frequency range of 200kHz-500Mhz) into cables that are characterized by a constant impedance and known velocity coefficient. If the pulse encounters a defect along the cable, a portion of the energy is reflected. The reflection time is used as an indication for the location of defects. Since in the case of carbon yarns, the velocity coefficient is not constant or known and since the impedance is length dependent, a calibration process is needed. The calibration process aims to correlate between the time and the actual location of the damage along the yarn.

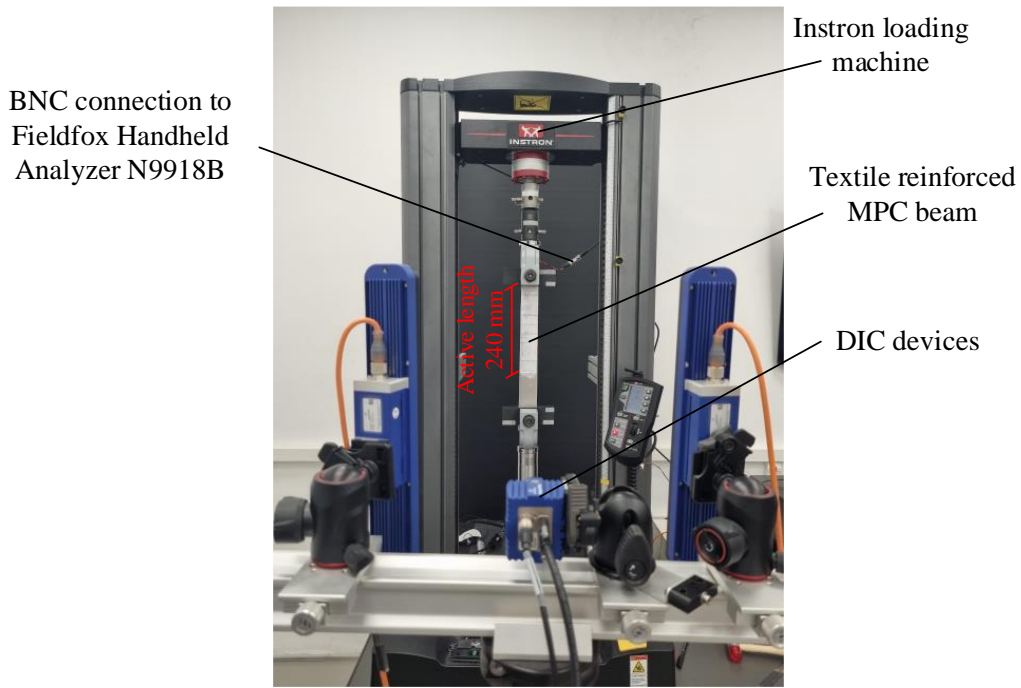


Figure 1. Loading setup.

The study offers a magnetic field-based calibration procedure, which is based on the fact that the magnet creates a local change in impedance. By knowing the location of the magnet and correlating it to the index of the extremum of the change of the spectrum of the impedance, a calibration function can be performed. Table I summarizes the correlation between several actual locations of the magnet with respect to the obtained extremum, named here identified index. It should be noted that this procedure was applied at the healthy state, before the any loading procedure was applied. The obtained calibration function is:

$$\text{Actual location [mm]} = 0.2215 * (\text{Identified index}) - 53.475 \quad (1)$$

TABLE I. DAMAGE INDEXES FOR EACH MAGNET LOCATION

Actual location [mm]	10	40	60	80	100	120	140	160	180	200
Identified Index [-]	252	422	516	632	709	796	893	964	1030	1120

The reflected spectrums of the impedance, measured every 1 sec, are the monitored values. The identification procedure explores the change of the spectrum of the impedance, that is the differences between two consecutive measurements. The study offers the following steps to identify the location of cracks:

Determining the noise level – It is done by measuring the maximum peak-to-peak (PTP) of the first 200 impedance spectrums change at an unloaded position. The

study offers a threshold value of 130% of the noise level. The noise level in our case is 0.019 [ $\Omega$ ] and the threshold value is 0.0247 [ $\Omega$ ].

Identifying the change of the spectrum of the impedance that have PTP value higher than the threshold value. If the PTP are associated with local maximum, they are classified as potential damage events, otherwise, they are not classified as potential events that should be considered.

Correlating the index and the identified local maximum to the location of cracks by the calibration function, see Eq. (1).

## RESULTS AND DISCUSSION

Results of the experimental test are presented in Fig. 2 and Fig. 3. Fig. 2 presents the load-deflection curve (Fig. 2a), the propagation of the cracks by the DIC analysis (Fig. 2b), and the PTP values of the impedance spectrum change (Fig. 2c). The threshold level of the PTP and the limit of interest (up to the ultimate load) are presented in the figure by dashed lines.

From Fig. 2a and 2b, it is seen that four cracks were formed. The formation of each crack defines an event that should be identified. The goal is to identify the occurrence of the events and their related crack locations.

From Fig. 2c it is seen that nine events were identified, they are marked in the figure. The identified events are associated to the identified PTP values that are higher than the threshold value.

According to the identification procedure only PTP values that have a local maximum, that is a local increase of the impedance, is considered as potential event. Exploring the nine events revealed that event #3 has no local maximum and accordingly is not considered in the identification procedure. This means that only events #1, #2, #4-#9 are considered as events that should be investigated.

The damage index is evaluated for the eight events, and the location of damage is calculated according to the calibration function, see Eq. 1. The locations of damage according to the identification procedure compared to the actual location (by the DIC technique) are presented in Fig. 3. It is seen that only event #1 was accurately identified. Both the location and the occurrence of the crack were successfully identified. It is further seen that the procedure identified the occurrence of events #2, #4, #5 and #7 but failed to detect their exact locations along the beam. It should be noted that the time of event #2 coincides with event #1, and it can be associated to the propagation of the crack within the beam cross-section. The reason for not detecting the exact location (of events #4, #5 and #7) is since the proposed calibration procedure considers only the effect of the change of the impedance within the yarn's length but ignore additional microstructural mechanism that occurs due to cracking.

Events #6, #8 and #9 are considered as false alarms since the events are not correlated to the formation of cracks. The false alarms can be considered to the inner micro-structural phenomena associated with the degradation of the filaments at the crack zones, either breakage of the sleeve filaments or extensive pull-out of the core ones.

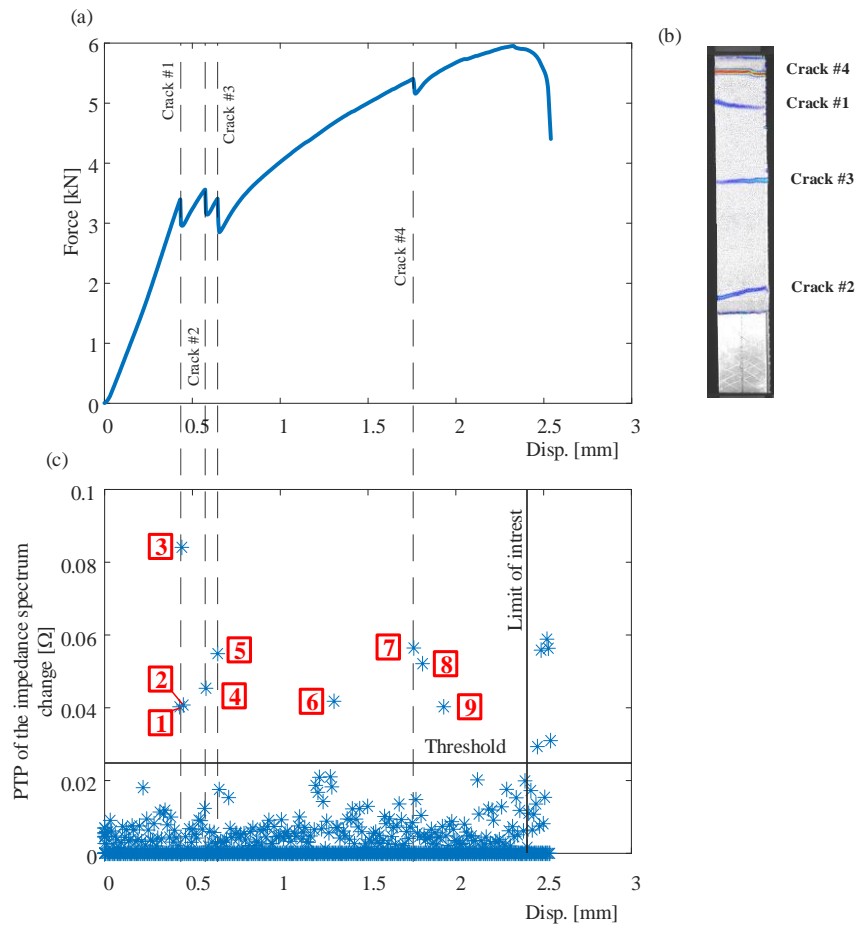


Figure 2. Mechanical response and TDR analysis: (a) Load- deflection curve; (b) Location of cracks by the DIC technique; (c) PTP values of the impedance spectrum changes versus deflection.

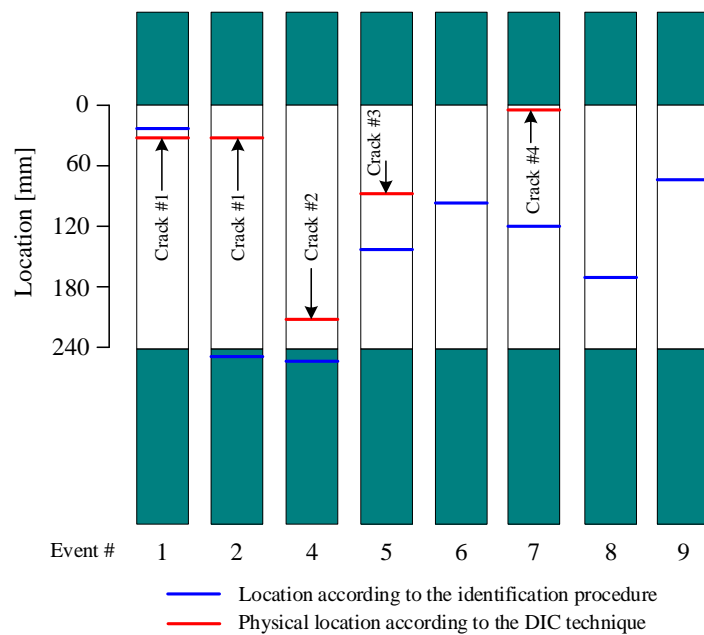


Figure 3. A comparison between the identified location of cracks versus the actual locations of cracks.

## CONCLUSIONS

This paper presented an initial demonstration of adopting the TDR analysis in identification procedures that locate damage along TRC elements. The procedure is based on exploring the change of the spectrum of the impedance, detecting the PTP values of the maximum of the change, and correlating the index of the maximum to actual location by calibration process. The study demonstrates the capabilities of the identification procedure by experimental investigation.

Carbon based textile reinforced MPC beam was loaded under uniaxial tensile loading and the identification procedure was applied. It was demonstrated that all damage events were detected using the proposed identification procedure but only the location of the first event was accurately identified. It is mainly associated with the calibration procedure that ignores micro-structural effects within the yarns that change the electrical and mechanical properties due to cracking. Furthermore, additional events were mistakenly identified and considered as false alarm. The false alarms are associated to inner degradation of the yarn at the location of the existing cracks.

This preliminary investigation demonstrates promising results that open the way for advanced investigations that will further bring the concept of self-sensory carbon yarns into realization.

## ACKNOWLEDGEMENTS

This research was supported by the ISRAEL SCIENCE FOUNDATION (grant No. 1663/21). The authors are thankful for the help of Eng. Barak Ofir and of the technical and administrative staff of the National Building Research Institute at the Technion. The authors acknowledge the support provided by ICL Group Ltd for providing the MPC mixture (Phosment) and by Teijin Frontier company Ltd for providing the short aramid fibers.

## REFERENCES

1. Christner, C., Horoschenkoff, A., Rapp, H., 2012. "Longitudinal and transvers strain sensitivity of embedded carbon fiber sensors," *Journal of Composite Materials.*, 47 (2): 155-167.
2. Gaben, M., Goldfeld, Y., 2022. "Self-sensory carbon-based textile reinforced concrete beams—Characterization of the structural-electrical response by AC measurements," *Sensors and Actuators A: Physical.*, 334: 113322.
3. Gaben, M., Goldfeld, Y., 2023. "Enhanced self-sensory measurements for smart carbon-based textile reinforced cement structures," *Measurement.*, 210 (2023): 112546.
4. Gaben, M., Goldfeld, Y., 2023. "Detecting damaged zones along smart self-sensory carbon based TRC by TDR," *Fibres and Textiles.*, 30(1): 54-60.
5. Goldfeld, Y., Yosef, L., 2019. "Sensing accumulated cracking with smart coated and uncoated carbon based TRC," *Measurement.*, 141: 137-151.
6. Yosef, L., Goldfeld, Y., 2020. "Smart self-sensory carbon-based textile reinforced concrete structures for structural health monitoring," *Structural Health Monitoring.*, 20(5):2396-2411.
7. Yosef, L., Goldfeld, Y., 2023. "Effect of matrix electrical and micro-structural properties on the self-sensory capabilities of smart textile reinforced composites," *Journal of Building Engineering.*, 67: 105909.
8. Goldfeld, Y., Perry, G., 2018. "Electrical characterization of smart sensory system using carbon based textile reinforced concrete for leakage detection," *Materials and Structures.*, 51(6): 170.

9. Shames, A., Horstmann, M., Hegger, J., 2014. "Experimental investigations on Textile-Reinforced Concrete (TRC) sandwich sections," *Composite Structures.*, 118, 643-653.
10. Wen, S., Wang, S., Chung, D. D. L., 1999. "Carbon fiber structural composites as thermistors," *Sensors and Actuators A: Physical.*, 78(2-3): 180-188.
11. De Andrade Silva, F., Butler, M., Mechtcherine, V., Zhu, D., Mobasher, B., 2011. "Strain rate effect on the tensile behavior of textile-reinforced concrete under static and dynamic loading," *Materials Science and Engineering: A.*, 528(3): 1727-1734.
12. Peled, A., Bentur, A. 2003. "Fabric structure and its reinforcing efficiency in textile reinforced cement composites," *Composites Part A: Applied Science and Manufacturing.*, 34(2): 107-118.
13. Soranakom, C., Mobasher, B., 2009. "Geometrical and mechanical aspects of fabric bonding and pullout in cement composites," *Materials and structures.*, 42(6): 765-777.
14. Perry, G., Dittel, G., Gries, T., Goldfeld, Y., 2021. "Monitoring capabilities of various smart self sensory carbon-based textiles to detect water infiltration," *Journal of Intelligent Material Systems and Structures.*, 32(20): 2566-2581.
15. Quadflieg, T., Stolyarov, O., Gries, T., 2016. "Carbon rovings as strain sensors for structural health monitoring of engineering materials and structures," *Journal of strain analysis for engineering design.*, 51(7): 482-492.